International Immunopharmacology 67 (2019) 239–247

Contents lists available at ScienceDirect

International Immunopharmacology

journal homepage: www.elsevier.com/locate/intimp

Effects of Platycodin D on S100A8/A9-induced inflammatory response in murine mammary carcinoma 4T1 cells

Yiyi Ye[a], Lixia Pei[a], Jing Ding[b], Chunyu Wu[c], Chenping Sun[c], Sheng Liu[a,c,*]

[a] Institute of Chinese Traditional Surgery, LongHua Hospital Shanghai University of Traditional Chinese Medicine, 725 Wanpingnan Road, Shanghai 200032, China
[b] Department of Pediatric Orthopaedics, Xinhua Hospital, School of Medicine, Shanghai Jiao Tong University, Shanghai 200092, China
[c] Department of Breast Surgery, LongHua Hospital Shanghai University of Traditional Chinese Medicine, 725 Wanpingnan Road, Shanghai 200032, China

ARTICLE INFO

Keywords:
Platycodin D
S100A8/A9
4T1 cells
Inflammation

ABSTRACT

Activation of the inflammatory signaling pathway is the most vital part of the pre-metastatic events of breast cancer. Platycodin D (PlaD) shows favorable pharmacological activities in anti-inflammatory and anti-tumor effect. The main purpose of this study was to survey the effects of PlaD on S100A8/A9-induced inflammation in mouse mammary carcinoma 4T1 cells. S100A8/A9 immunolocalization and expression in pre-metastatic lung tissue were assessed by immunofluorescence staining and ELISA. 4T1 cells were treated with 2.5 μg/mL recombinant S100A8/A9 heterodimer and 7.5, 10, or 12.5 μM of PlaD. After 24 h of incubation, cell viability, migration, and invasion were evaluated by CCK-8, wound-healing, and transwell assay, respectively. Nuclear translocation of NF-κB p65 was determined by immunostaining and western blot. The levels of pro-inflammatory cytokines including IL-1β, IL-6, and TNF-α were detected by ELISA. The results showed that S100A8/A9 was actively increased and released into the extracellular space during the pre-metastatic phase of breast cancer. PlaD treatment attenuated S100A8/A9-induced growth, migration, and invasion of 4T1 cells. Furthermore, PlaD decreased the levels of IL-1β, IL-6, and TNF-α by inhibiting nuclear translocation of NF-κB p65. In conclusion, this study demonstrated that PlaD inhibited S100A8/A9-induced inflammatory response in 4T1 cells by suppressing the expression of IL-6, IL-1β, and TNF-α via inhibition of NF-κB signaling pathways.

1. Introduction

Breast cancer, a serious threat to women's health, was the most frequently diagnosed cancer in the female all around the world [1,2]. Distant metastasis, the leading cause of death in patients with breast cancer, includes bone, lung, liver, and brain, among which lung metastasis is one of the most frequent organ metastases [3].

Pre-metastatic niche acts a pivotal part in tumor metastasis to specific organs. Primary tumor and target organs work together to establish the pre-metastatic niche, promoting the process of lung metastasis [4,5]. A recent study has shown that neutrophils in bone marrow-derived cells (BMDCs) create an inflammatory microenvironment that promotes metastasis by inhibiting innate and secondary anti-tumor immune responses [6]. It is believed that vascular endothelial growth factor (VEGF), macrophage-colony stimulating factor (M-CSF), and tumor necrosis factor α (TNF-α), which are secreted by the melanoma before the tumor metastases to the lung, induced inflammatory cell aggregation in the pre-metastatic niche [7]. Similarly, our previous study showed that lymphocyte mass existed in lung tissue before metastasis, indicating that lymphocytes were associated with the establishment of the pre-metastatic niche [8].

In summary, activation of the inflammatory signaling pathways is one of the essential pre-metastatic events. S100A8, S100A9, and S100A8/A9 heterodimers are calcium-binding proteins that play extracellular pro-inflammatory functions and participate in the entire process of pre-metastatic events [9–11]. During the pre-metastasis period, the expression of S100A8 and S100A9 in the lung was significantly increased under host effect. These factors recruit a large number of BMDCs to gather in the lung before metastasis and form a pre-metastatic microenvironment similar to an inflammatory state, which is suitable for tumor cell adhesion and infiltration [12]. The stability of S100A8/A9 heterodimer is better than that of S100A8 and S100A9, so the pro-inflammatory effect of S100A8 and S100A9 is often attributed to their heterodimer [13]. Since the abnormal expression of S100A8/A9 in microenvironment before metastasis, it may contribute to the survival, proliferation, migration, and invasion of circulating

* Corresponding author at: Institute of Chinese Traditional Surgery, LongHua Hospital Shanghai University of Traditional Chinese Medicine, 725 Wanpingnan Road, Shanghai 200032, China.
E-mail address: yige823@163.com (S. Liu).

https://doi.org/10.1016/j.intimp.2018.12.008
Received 22 August 2018; Received in revised form 3 December 2018; Accepted 4 December 2018
Available online 15 December 2018
1567-5769/

tumor cells in lung tissue.

According to the literature reported, as a major triterpene saponin extracted from the roots of *Platycodon grandiflorum*, Platycodin D (PlaD) shows favorable pharmacological activities in anti-inflammatory and anti-tumor effect [14]. PlaD attenuated interleukin 1β (IL-1β)-induced inflammatory response in osteoarthritis chondrocyte by activating LXRα [15]. PLaD prevented inflammation caused by LPS through the LXRα–ABCA1 signaling pathway, which not only disrupted lipid rafts, but also prevented TLR4 translocation into lipid rafts [14]. Wang's results confirmed that PlaD inhibited IL-13-induced the expression of inflammatory cytokines and mucus in nasal epithelial cells by inhibiting the activation of nuclear factor κB (NF-κB) and mitogen-activated protein kinase (MAPK) signaling pathways [16]. PlaD potentiated proliferation inhibition and apoptosis induction upon AKT inhibition via feedback blockade in non-small cell lung cancer cells [17]. However, the anti-inflammatory effects of PlaD in the pre-metastatic lung of breast cancer have not been deeply investigated. In the present study, we sought to explore the effects of PlaD on S100A8/A9-induced inflammation in murine mammary carcinoma 4T1 cells.

2. Materials and methods

2.1. Compounds

PlaD (purity ≥ 98%, HPLC grade) was obtained from Sichuan Weikeqi Biological Technology Co., Ltd (Sichuan, China). The structure of PlaD is presented in Fig. 1.

2.2. Cell culture

The murine mammary carcinoma 4T1 cell line was purchased from the Cell Bank of Type Culture Collection of the Chinese Academy of Sciences (Shanghai, China). The cells were cultured in RPMI-1640 medium (Gibco-Invitrogen, NY, USA) containing 10% fetal bovine serum (FBS, Gibco-Invitrogen) at 37 °C in a 5% CO_2 humidified chamber.

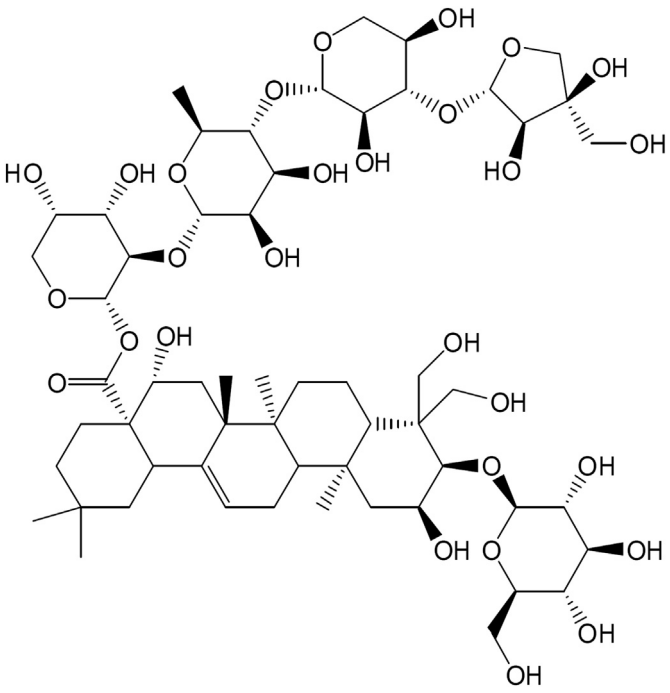

Fig. 1. Structure of PlaD.

2.3. Animals and experimental pre-metastatic model

Female BALB/c mice, aged five weeks, were purchased from SLAC Laboratory Animal Co. Ltd, (Shanghai, China) and raised in individual cages under specific-pathogen-free (SPF) level in the Department of Laboratory Animal Science, Fudan University. The mice were allowed to acclimate for 7 days before inoculation and were fed with tap water and standard laboratory diet. All animal experiments were conducted following the animal experimental guidelines set by the National Institutes of Health Guide for the Care and Use of Laboratory Animals.

The 4T1 cells were harvested, and the suspension concentration was adjusted to 2×10^6 cells/mL. Except for the control group, the cells in a volume of 100 μL were injected into the fourth mammary fat pads on the right side of BALB/c mice. According to the previous experimental results [8], day 0 to day 14 was the pre-metastatic stage. On day 14, although tumor cells were not obvious, microenvironment changes were observed in the lungs. Therefore, day 14 was selected for subsequent tests.

2.4. S100A8/A9 immunolocalization and expression in pre-metastatic lung tissue

Fourteen days after 4T1 implantation, mice were euthanized, and the lung was perfused with 4% cold formaldehyde. Next, the lung tissues were post-fixed in 4% formaldehyde overnight. Specimens were dehydrated with graded alcohol before paraffin embedding. Then, embedded tissues were cut into 5 μm sections and undergone double-labeling immunofluorescence staining and immunohistochemistry (IHC). After blocking with 1% bovine serum albumin, sections were incubated with the anti-S100A8/A9 antibody (1:100 dilution, Abcam, Cambridge, UK) overnight and immunolabeled with Alexa Fluor 488 affinipure donkey anti-mouse IgG (H + L) antibody (1:200 dilution, Yeasen, Shanghai, China) for 60 min. Sections were stained with DAPI (Beyotime Biotechnology, Jiangsu, China) for nuclear counterstaining, and the sample slides were imaged using the LSM 800 confocal laser scanning microscopy (Zeiss, Germany).

For the IHC, sections were blocked with 1% bovine serum albumin, incubated with the anti-S100A8/A9 antibody (1:150 dilution, Abcam) overnight, and then incubated with the HRP-labeled goat anti-mouse IgG (H + L) antibody (1:50 dilution, Beyotime Biotechnology) for 50 min. After DAB staining and hematoxylin counterstaining, sections were dehydrated with graded alcohol, hyalinized in xylene, and finally sealed with neutral gum. Under the microscope, the positive cells were stained brown.

For S100A8/A9 measurement, supernatants were obtained by centrifugation after homogenization of lung tissues with sample homogenizer (FastPrep-24, MP, USA). The sample protein concentration was quantified using the BCA assay kit (Beyotime Biotechnology). The levels of S100A8/A9 were measured using an ELISA kit (R&D system, MN, USA), according to the manufacturer's instructions.

2.5. Cell viability assay

Concentration-response curves and half maximal inhibitory concentration (IC50) were determined using the cell counting kit-8 (CCK-8, Beyotime Biotechnology). Cells (2×10^5 cells/mL) were seeded in 96-well plates and incubated for 12 h. PlaD was diluted to appropriate concentrations (10, 12.5, 15, 20, and 25 μM) and immediately applied to the cells. To test whether recombinant mouse S100A8/A9 heterodimer (R&D system) would enhance or inhibit the viability, cells were treated with 2.5 μg/mL of S100A8/A9 and incubated with plaD in combination. After 24 h of exposure, cell viability was evaluated by CCK-8. The absorbance values were detected at 450 nm, and the IC50 value was extrapolated using linear regression analysis.

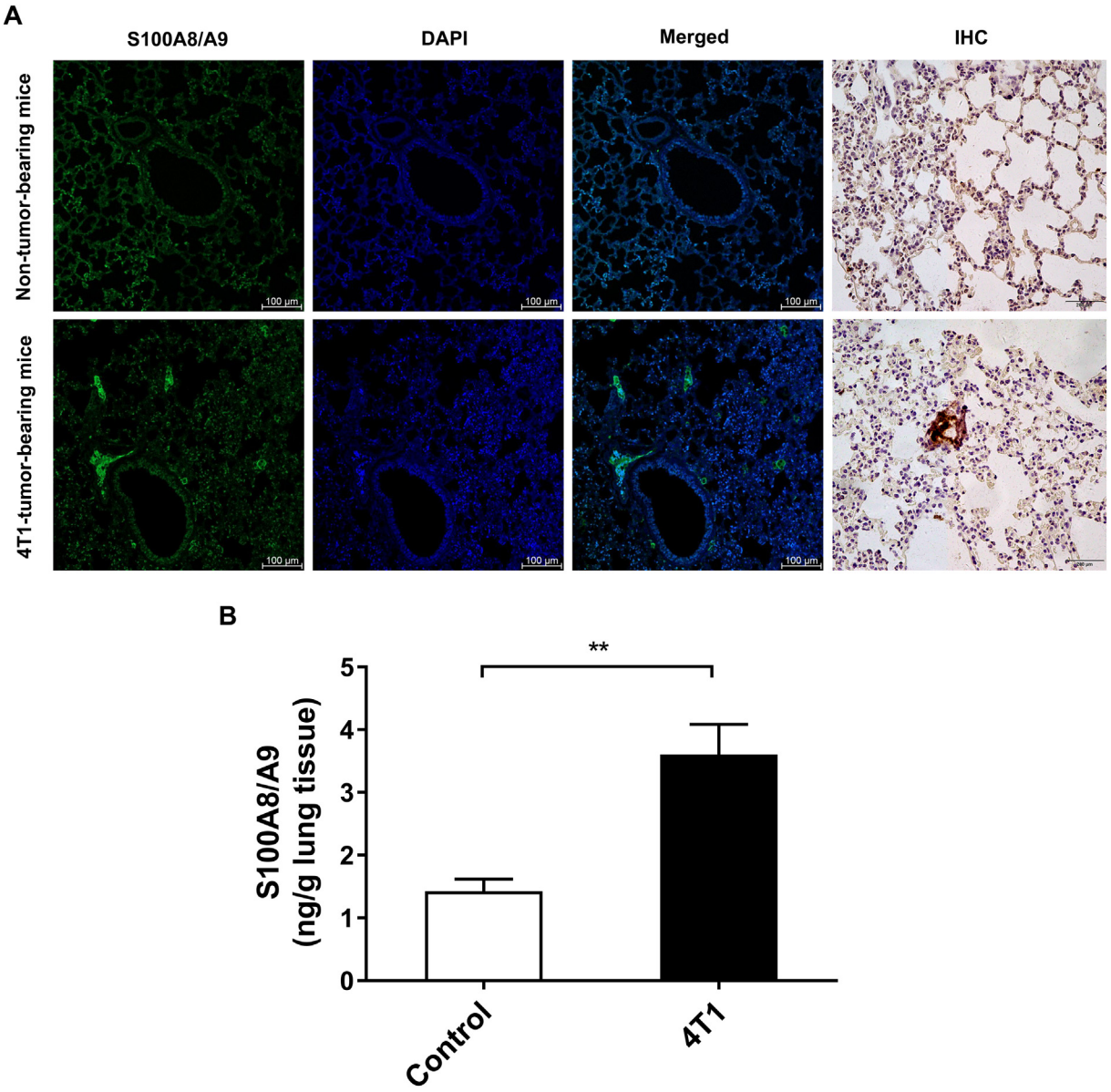

Fig. 2. S100A8/A9 immunolocalization and expression in pre-metastatic lung tissue. A, Release of S100A8/A9 from the cytosol into the extracellular space in the pre-metastatic lungs. Lung tissues were undergone double-labeling immunofluorescence staining and IHC. Imaging shown is representative of three experiments with similar results. Green, S100A8/A9 heterodimer; blue, nucleus; scale bar, 100 μm for immunofluorescence and 200 μm for IHC. B, The expression of S100A8/A9 in pre-metastatic lung tissue was detected by ELISA. Each bar represents mean ± SD (n = 5), and *p*-values were obtained with one-way ANOVA followed by Dunnett's post hoc test. **, $p < 0.01$. (For interpretation of the references to color in this figure legend, the reader is referred to the web version of this article.)

2.6. Cell migration assay

Cells (2×10^5 cells/mL) were seeded in 6-well plates and cultured to 90% fusion. The cell monolayers were scraped with a sterile pipette tip to form a gap. Wells were then rinsed with PBS to remove any free-floating cells and debris, and replaced with serum-free medium containing 2.5 μg/mL of S100A8/A9 and different concentrations of PlaD. Cells were photographed at 0 and 24 h, and the percentage of wound-healing was calculated as follows: wound-healing percentage = (original wound area − remaining wound area) / original wound area × 100.

2.7. Cell invasion assay

Cell invasive ability was performed with 24-well transwell plates equipped with the 8 μm pore in polyethylene terephthalate membranes (Corning Life Sciences, NY, USA) [18]. Matrigel (Corning Life Sciences) was diluted (1:30) with pre-cooled coating buffer (0.01 M Tris (pH 8.0), 0.7%NaCl) and added to the pre-cooled filter to form a thin gel layer. Cells were incubated for 24 h with S100A8/A9 and PlaD, alone or in combination. Afterward, cells were harvested and suspended at a density of 2×10^5 cells/mL in 100 μL of serum-free 1640 medium and then seeded into the upper chamber. The lower chamber was filled with 600 μL of medium with 10% FBS. After incubation for 24 h at 37 °C in a CO_2 incubator, the cells on the upper surface of the filter were removed using a cotton swab. Cells that invaded to the lower surface were stained with DAPI and counted using the LSM 800 confocal laser scanning microscopy.

2.8. Nuclear translocation of NF-κB p65

Activation of NF-κB can be determined by immunostaining if p65,

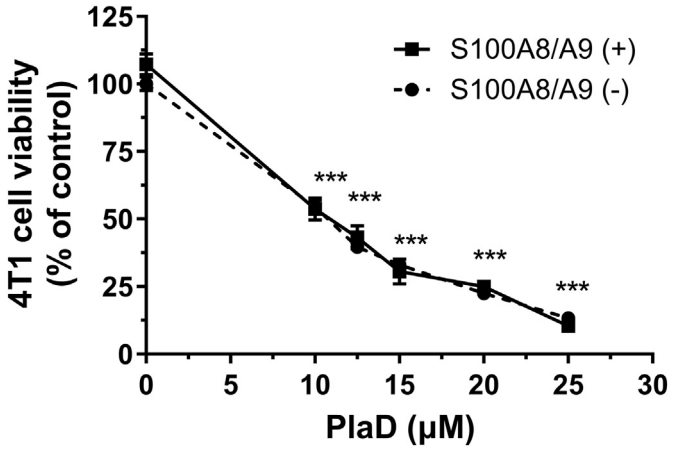

Fig. 3. Effects of PlaD on cell viability of 4T1 in the presence of S100A8/A9 or not. Cells were treated with S100A8/A9 (2.5 μg/mL) and PlaD (10, 12.5, 15, 20, and 25 μM) for 24 h, and cell viability was assessed by CCK-8. Cells untreated with PlaD were considered as the control group. Results are expressed as mean ± SD of three separate experiments performed in triplicate, and *p*-values were obtained with one-way ANOVA followed by Dunnett's post hoc test. ***, $p < 0.001$ vs. the control group.

the main subunit of NF-κB, was transferred to the nucleus. Cells (2×10^5 cells/mL) were seeded in confocal plates and incubated for 12 h. Next, cells were treated with 2.5 μg/mL of S100A8/A9, alone or in combination with 7.5, 10, 12.5 μM of PlaD for the further 24 h. Nuclear translocation of NF-κB p65 was detected using the NF-κB activation and nuclear translocation assay kit (Beyotime Biotechnology) according to the manufacturer's instructions. Briefly, cells were fixed with fixing solution for 15 min, rinsed with washing solution, and overlaid with blocking liquid for 1 h. Then cells were incubated with NF-κB p65 antibody at 4 °C overnight. The next day, cells were incubated with Cy3-conjugated anti-rabbit antibody for 1 h and then stained with DAPI for 5 min. Finally, the localization of NF-κB p65 was visualized using a confocal laser scanning microscopy (LSM 800).

2.9. Protein isolation and western blot analysis

Total cellular proteins were isolated using a cell lysis buffer, and the protein concentration was quantified using the BCA assay kit (Beyotime Biotechnology). The total proteins were electrophoresed using sodium dodecyl sulfate-polyacrylamide gel electrophoresis and transferred to nitrocellulose membranes. The membranes were blocked using 5% nonfat milk for 1 h and incubated overnight at 4 °C with NF-κB antibody (dilution 1:1000; Cell Signaling Technology, Inc., Boston, USA) and GAPDH antibody (dilution 1:1000, Proteintech, Hubei, China). After being rinsed, the membranes were incubated with 1:500 dilute solution of HRP-labeled goat anti-rabbit IgG (H + L) (Beyotime Biotechnology) for 1 h. The blots were visualized with enhanced-chemiluminescence using BeyoECL Plus Kit (Beyotime Biotechnology). GAPDH served as the loading control.

2.10. Enzyme-linked immunosorbent assay (ELISA)

Cells (2×10^5 cells/mL) were seeded in 6-well plates and incubated for 12 h. Next, cells were treated with 2.5 μg/mL of S100A8/A9, alone or in combination with 7.5, 10, 12.5 μM of PlaD for the further 24 h. After S100A8/A9 stimulation and PlaD treatment, culture supernatant from each well was collected. The levels of IL-1β, IL-6, and TNF-α in the supernatants were measured using ELISA kits (Beyotime Biotechnology), according to the manufacturer's instructions. Briefly, 100 μL of diluent standards and samples was added to appropriate wells and incubated at 37 °C for 2 h. After that, 100 μL of antibody was added to all wells and wells were incubated at 37 °C for 1 h. After washed each well, 100 μL of streptavidin-HRP was added and wells were incubated at 37 °C for 30 min. Nest, after the tetramethylbenzidine substrate was added, the wells were incubated at 37 °C for 20 min in a dark place. Finally, the reaction was terminated by adding 50 μL of stop solution and absorbance was measured spectrophotometrically using a microplate reader (Synergy H1, BioTek, USA). The final concentrations of IL-1β, IL-6, and TNF-α were calculated using the standard curve.

2.11. Statistical analysis

Data were presented as mean ± standard deviation (SD). Differences of the data among and between groups were analyzed with one-way analysis of variance (ANOVA) followed by Dunnett's post hoc test. $p < 0.05$ were considered to indicate a statistically significant difference.

3. Results

3.1. The release of S100A8/A9 from the cytosol into the extracellular space in the pre-metastatic lungs

S100A8/A9 is increased significantly in many inflammatory processes, and this heterodimer has been used as an inflammatory biomarker for many years [19]. In the present study, we found the release of S100A8/A9 into the extracellular space in the lungs of 4T1-tumor-bearing mice (Fig. 2A). Extracellular S100A8/A9 was absent or was present at low levels in lungs from non-tumor mice (Fig. 2A). Moreover, S100A8/A9 levels were increased approximately 2.5-fold in tumor mice ($p < 0.01$) compared to non-tumor-bearing mice (Fig. 2B). These findings suggested that S100A8/A9 may in fact be actively increased and released into the extracellular space during the pre-metastatic phase. Our previous studies showed an inflammatory response leading to the abnormity of the pulmonary microenvironment during the pre-metastatic phase [8]. Indeed, the S100A8/A9 complex was released during inflammatory events and exerted its pro-inflammatory effect, which was consistent with our previous conclusion.

3.2. Effects of PlaD on cell viability of 4 T1 in the presence of S100A8/A9

As shown in Fig. 3, in the range of 10–25 μM, PlaD had a significant inhibitory effect on 4T1 cells ($p < 0.001$), and this effect was enhanced by the increase in concentration. The IC50 value of PlaD was 10.7 μM. According to the experimental results, the concentrations of 7.5, 10, and 12.5 μM were chosen for use in all subsequent assays. Moreover, it was found that S100A8/A9 at 2.5 μg/mL had no obvious inhibition or activation effect on 4T1 cells. Similarly, 2.5 μg/mL of S100A8/A9 had no impact on the inhibition of PlaD on 4T1, regardless of the concentration of PlaD.

3.3. Treatment of PlaD attenuated S100A8/A9-induced migration of 4T1 cells

To determine whether recombined protein S100A8/A9 induces migration in 4T1 cells, the wound-healing assay was performed. The cell density of migration assay (cells were incubated until the cell grows to 90% fusion) was greater than that of the CCK-8 experiment, so the inhibitory effect of PlaD was changed. In addition, we use the serum-free medium in which cells are difficult to proliferate. If PlaD inhibited cell survival, the wound area should be larger after 24 h, but in fact the remaining wound area is smaller than the original wound area, and the wound-healing percentage is lower than that of the S100A8/A9-induced group, indicating PlaD inhibited the migration of cells.

The addition of 2.5 μg/mL S100A8/A9 sharply increased the migration ability of 4T1 cells from 39.57% to 55.06% ($p < 0.05$). After treatment with PlaD, migration inducing effect of S100A8/A9 was

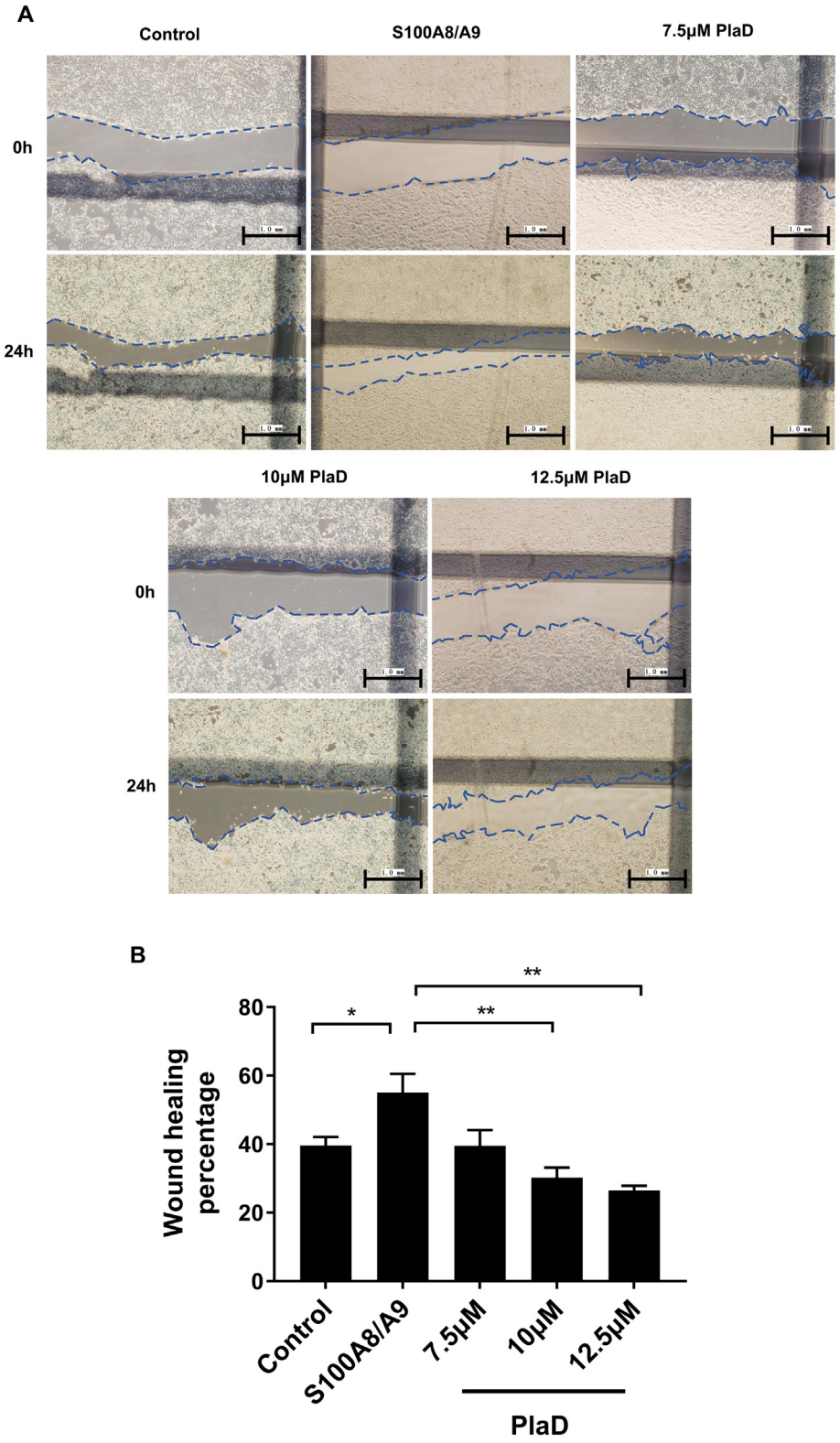

Fig. 4. Treatment of PlaD attenuated S100A8/A9-induced migration of 4T1 cells. A, Photomicrographs of cell migration from the wound-healing assay. Imaging shown is representative of three experiments with similar results. Scale bar, 1 mm. B, Wound-healing percentage of 4T1 cells after treated with S100A8/A9, alone or in combination with PlaD. Each bar represents mean ± SD (n = 3), and *p*-values were obtained with one-way ANOVA followed by Dunnett's post hoc test. *, $p < 0.05$; **, $p < 0.01$.

significantly inhibited ($p < 0.01$). The inhibitory effect of 10 μM group and 12.5 μM group was stronger and more obvious, which was in a concentration-dependent manner (Fig. 4).

3.4. Treatment of PlaD attenuated S100A8/A9-induced invasion of 4T1 cells

To determine whether recombined protein S100A8/A9 induces

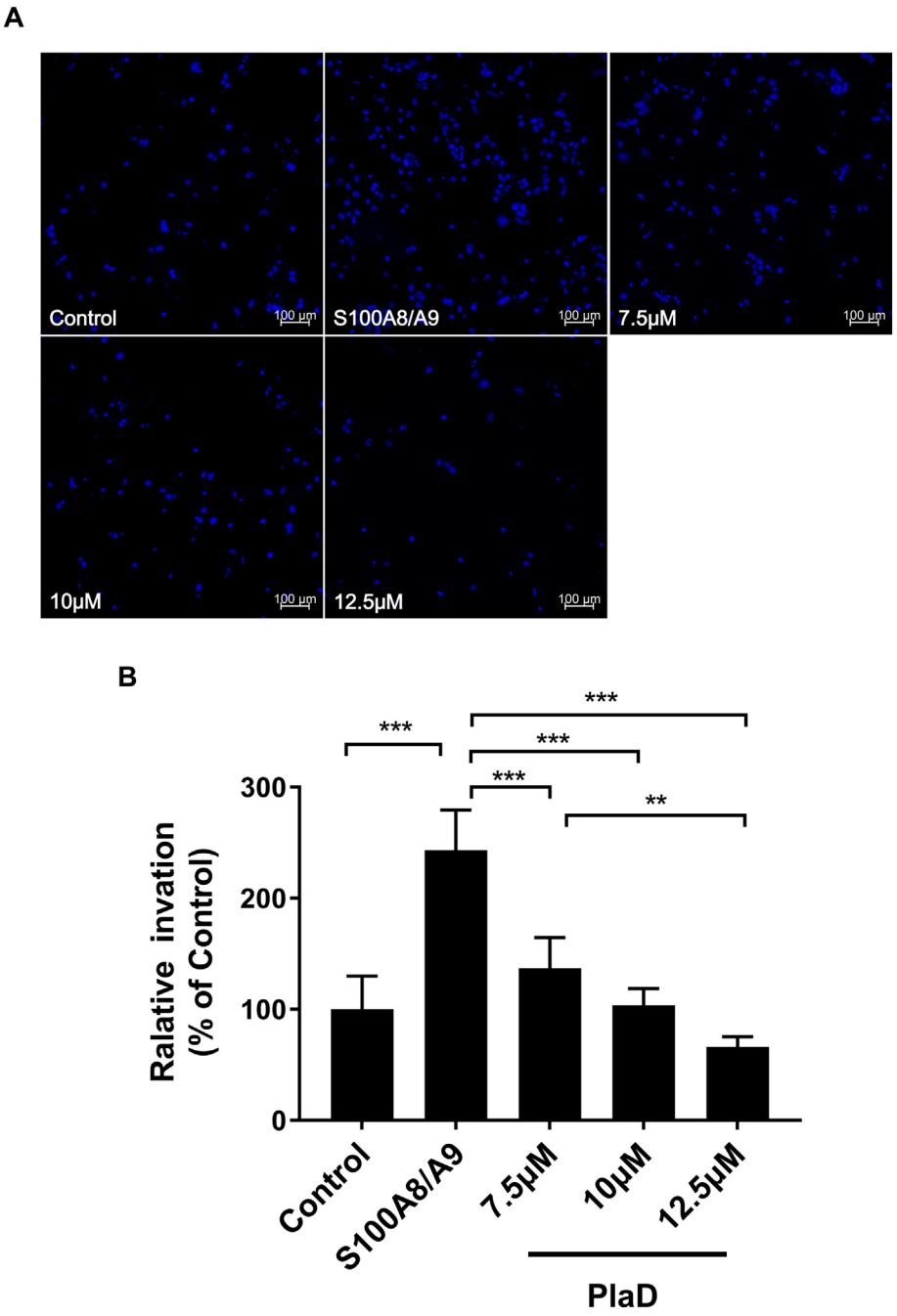

Fig. 5. Treatment of PlaD attenuated S100A8/A9-induced invasion of 4T1 cells. A, Photomicrographs of cell invasion from transwell assays. Imaging shown is representative of three experiments with similar results. Blue, nucleus; scale bar, 100 μm. B, Relative invasion percentage of 4T1 cells after treated with S100A8/A9, alone or in combination with PlaD. Cells were counted in 8 randomly selected fields. Each bar represents mean ± SD (n = 3), and *p*-values were obtained with one-way ANOVA followed by Dunnett's post hoc test. **, $p < 0.01$; ***, $p < 0.001$. (For interpretation of the references to color in this figure legend, the reader is referred to the web version of this article.)

invasion in 4T1 cells, transwell assay was performed. The cells were intervened by plaD, and next they were adjusted to a uniform concentration (2×10^5 cells/mL) before being seeded into the upper chamber of the transwell insert. As seen in Fig. 5, the invasion capacity of 4T1 cells was greatly enhanced by 2.5 μg/mL S100A8/A9 exposure (from 100% to 243%, $p < 0.001$), but the invasion rate was significantly decreased after PlaD treatment ($p < 0.001$). Moreover, a concentration-dependent inhibitory effect was observed in PlaD group. Treatment of 7.5 μM PlaD significantly decreased the invasion ability to 136% ($p < 0.001$), the 10 μM PlaD group reduced to about half of the invasion rate compared to S100A8/A9 group (103.64%, $p < 0.001$), and the inhibitory effect of 12.5 μM group (66.11%) was better than that of the 10 μM group.

3.5. Treatment of PlaD inhibited S100A8/A9-induced nuclear translocation of NF-κB p65

Western blot result (Fig. 6B and C) showed that there was no significant difference in the expression of total p65 in each group ($p > 0.05$). Compared with the normal control group, NF-κB p65 nuclear translocation in S100A8/A9 group was significantly increased. After the intervention of PlaD, the NF-κB p65 nuclear translocation in each concentration group was reduced, and the inhibitory effect of 10 μM and 12.5 μM group was further enhanced compared with the 7.5 μM group (Fig. 6A).

3.6. Treatment of PlaD inhibited S100A8/A9-induced over-expressions of IL-1β, IL-6, and TNF-α

To determine the effect of S100A8/A9 on pro-inflammatory

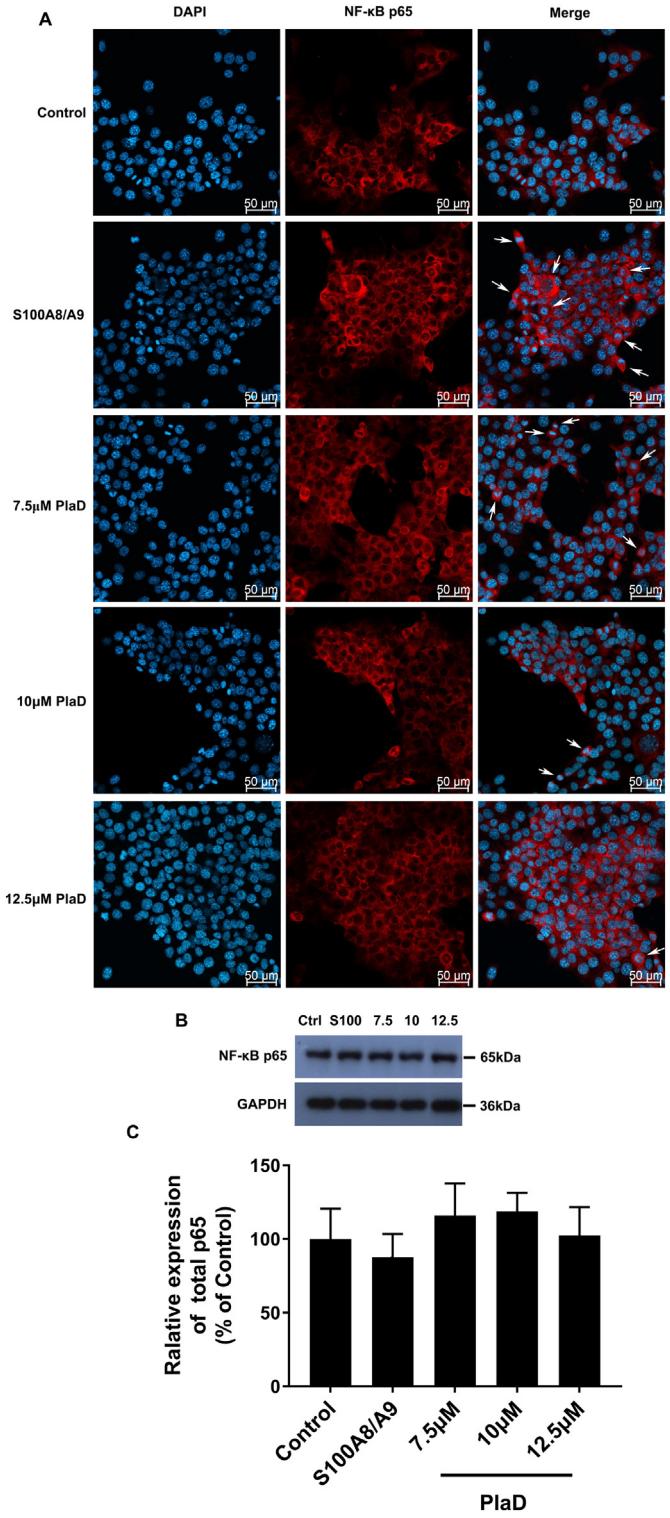

Fig. 6. Treatment of PlaD inhibited S100A8/A9-induced nuclear translocation of NF-κB p65. A, Photomicrographs of NF-κB p65 localization. Imaging shown is representative of three experiments with similar results. Red, NF-κB p65; blue, nucleus; scale bar, 50 μm. B, Representative image of blots. GAPDH served as the loading control. C, The relative abundance of each band. Scanning densitometry was used for semi-quantitative analysis in comparison to the control group. Each bar represents mean ± SD (n = 3), and *p*-values were obtained with one-way ANOVA followed by Dunnett's post hoc test. (For interpretation of the references to color in this figure legend, the reader is referred to the web version of this article.)

cytokines including IL-1β, IL-6 and TNF-α, and the anti-inflammatory effect of PlaD, 4T1 cells were treated with 2.5 μg/mL of S100A8/A9 and intervened with various concentrations of PlaD. As we expected, the recombinant protein S100A8/A9 significantly mobilized the expressions of IL-1β, IL-6, and TNF-α (Fig. 7, $p < 0.001$). After treatment with PlaD, the over-expressions of these inflammatory factors were decreased in a concentration-dependent manner (Fig. 7, $p < 0.05$).

4. Discussion

The increase in vascular permeability and activation of inflammatory signaling pathway are the typical initiation events of microenvironment formation of pre-pulmonary metastasis [12]. Our previous study [8] found that pulmonary vascular permeability and capillary telangiectasia were increased in 4T1-tumor-bearing mice compared with normal mice. Besides, we also observed lymphocytic infiltration in the pre-metastatic lung tissues. In the initial stage of inflammation, the activation of inflammatory factors could induce vasodilation and hyperpermeability of the vessel. Therefore, we believe that inflammation and inflammation-induced vascular hyperpermeability lay the foundation for pulmonary microenvironmental abnormalities during the pre-metastatic period of breast cancer.

The heterogeneous dimer S100A8/A9, mainly derived from neutrophils and monocytes, is the activator of the innate immune system [20]. S100A8/A9 is involved in the whole process of metastasis, and plays a pivotal role in the establishment of the pre-metastatic microenvironment, increases the migration ability of tumor cells, and accelerates the occurrence of pulmonary metastasis [6,21]. The expressions of S100A8 and S100A9 in the lung increased dramatically in the stage of pre-metastasis. These factors recruit a large number of bone marrow cells, hematopoietic precursors, and macrophages to gather in the pre-metastatic lung [12,22]. Our in vivo study demonstrated the release of S100A8/A9 into the extracellular space during the pre-metastatic phase. The inflammatory role of extracellular S100A8/A9 induced abnormal microenvironment of lung tissue, which may be one of the principal causes of pulmonary metastasis in breast cancer. Indeed, our in vitro data indicated that although the addition of recombinant protein S100A8/A9 did not alter the survival of 4T1 tumor cells, it greatly improved the migration and invasion ability of 4T1 cells.

Extracellular S100A8/A9 affects multiple steps of leukocyte recruitment by binding to surface receptors including Toll-like receptor-4 (TLR-4) and the receptor of advanced glycation endproducts (RAGE) [23,24]. These give rise to the induction of NF-κB, and eventually lead to the releases of pro-inflammatory factors [25,26]. Herein, we evaluated the role of recombinant protein S100A8/A9 on the expressions of pro-inflammatory factors such as IL-1β, IL-6, and TNF-α in vitro. IL-6 and IL-1β are important inflammatory regulatory factors. These two proteins are also associated with tumor growth and metastasis. IL-1β is one of the main subtypes of the IL-1 family, which mediates the important process of inflammation, and it is also one of the important components in the inflammatory microenvironment, which is associated with the occurrence, development, and metastasis of many types of tumors [26]. IL-6 controls the morphological changes of tumor cells and participates in epithelial-mesenchymal transition [27]. TNF-α is a multipotent cytokine that causes cell proliferation, cell death, and inflammation. In addition to the cytotoxic effect on cancer cells, TNF-α also plays a tumor-promoting activity. Abnormal TNF-α signal promotes tumor cell motility, invasion, and tumor metastasis [28]. The addition of recombinant protein S100A8/A9 led to the inductions of TNF-α, IL-6, and IL-1β in our experiment. Also, we found that cell motility enhancement mediated by these pro-inflammatory factors was caused by activation of the NF-κB signaling pathway.

According to the latest report, PlaD possesses anti-inflammatory and anti-tumor capacity [15,17]. Earlier studies provided evidence that PlaD inhibited migration, invasion, and growth of tumor cells and decreased the expressions of inflammatory cytokines by suppressing the

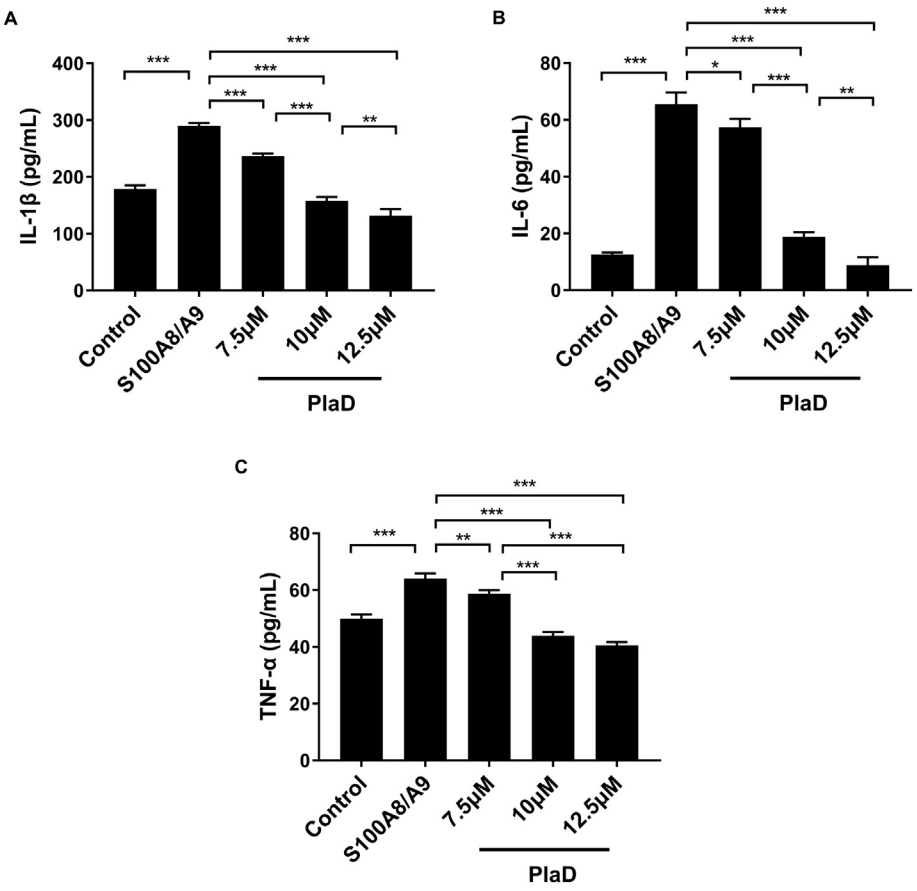

Fig. 7. Treatment of PlaD inhibited S100A8/A9-induced over-expressions of IL-1β, IL-6, and TNF-α. The levels of IL-1β (A), IL-6 (B) and TNF-α (C) were detected by ELISA. Each bar represents mean ± SD (n = 3), and *p*-values were obtained with one-way ANOVA followed by Dunnett's post hoc test. *, $p < 0.05$; **, $p < 0.01$; ***, $p < 0.001$.

activation of NF-κB signaling pathways [16,29]. Consequently, we conjectured that the anti-inflammatory and anti-tumor effects of PlaD on S100A8/A9-stimulated 4T1 cells might also be relevant to NF-κB signaling pathway. Our experiments demonstrated that PlaD attenuated S100A8/A9-induced TNF-α, IL-6, and IL-1β over-expressions in 4T1 cells by inhibiting nuclear translocation of NF-κB p65, and finally suppressed the ability of cell growth, migration, and invasion in a dose-dependent manner.

In conclusion, we have shown that S100A8/A9, a sensitive local and systemic marker for the detection of inflammatory activity, promoted growth, migration, and invasion of highly metastatic 4T1 mammary carcinoma cells. PlaD suppressed the generation of pro-inflammatory cytokines including IL-6, IL-1β, and TNF-α via inhibition of NF-κB signaling pathways, and eventually inhibited inflammatory response of cancer. Based on our results, PlaD might be conducive to the treatment of breast cancer metastasis.

Acknowledgments

The authors are grateful for financial supports from the Natural Science Foundation of Shanghai (No. 17ZR1430700 and 17ZR1430900) and the 2018–2020 Three-year Action Plan for Traditional Chinese Medicine Further Development in Shanghai (No. ZY (2018-2020)-CCCX-2002-10).

Conflict of interest

The authors declare that they have no competing interests.

References

[1] L.A. Torre, F. Bray, R.L. Siegel, J. Ferlay, J. Lortet-Tieulent, A. Jemal, Global cancer statistics, 2012, CA Cancer J. Clin. 65 (2) (2015) 87–108, https://doi.org/10.3322/caac.21262.
[2] W. Chen, R. Zheng, S. Zhang, H. Zeng, C. Xia, T. Zuo, Z. Yang, X. Zou, J. He, Cancer incidence and mortality in China, 2013, Cancer Lett. 401 (2017) 63–71, https://doi.org/10.1016/j.canlet.2017.04.024.
[3] A.W. Lambert, D.R. Pattabiraman, R.A. Weinberg, Emerging biological principles of metastasis, Cell 168 (4) (2017) 670–691, https://doi.org/10.1016/j.cell.2016.11.037.
[4] D.F. Quail, J.A. Joyce, Microenvironmental regulation of tumor progression and metastasis, Nat. Med. 19 (11) (2013) 1423–1437, https://doi.org/10.1038/nm.3394.
[5] J. Ursini-Siegel, P.M. Siegel, The influence of the pre-metastatic niche on breast cancer metastasis, Cancer Lett. 380 (1) (2016) 281–288, https://doi.org/10.1016/j.canlet.2015.11.009.
[6] C.F. Wu, L. Andzinski, N. Kasnitz, A. Kroger, F. Klawonn, S. Lienenklaus, S. Weiss, J. Jablonska, The lack of type I interferon induces neutrophil-mediated pre-metastatic niche formation in the mouse lung, Int. J. Cancer 137 (4) (2015) 837–847, https://doi.org/10.1002/ijc.29444.
[7] M. Han, J. Xu, Y. Bi, M. Jiang, X. Xu, Q. Liu, J. Jia, Primary tumor regulates the pulmonary microenvironment in melanoma carcinoma model and facilitates lung metastasis, J. Cancer Res. Clin. Oncol. 139 (1) (2013) 57–65, https://doi.org/10.1007/s00432-012-1299-7.
[8] Y. Ye, S. Liu, C. Wu, Z. Sun, TGFbeta modulates inflammatory cytokines and growth factors to create premetastatic microenvironment and stimulate lung metastasis, J. Mol. Histol. 46 (4–5) (2015) 365–375, https://doi.org/10.1007/s10735-015-9633-4.
[9] E. Lukanidin, J.P. Sleeman, Building the niche: the role of the S100 proteins in metastatic growth, Semin. Cancer Biol. 22 (3) (2012) 216–225, https://doi.org/10.1016/j.semcancer.2012.02.006.
[10] H. Chen, C. Xu, Q. Jin, Z. Liu, S100 protein family in human cancer, Am. J. Cancer Res. 4 (2) (2014) 89–115.
[11] K. Drews-Elger, E. Iorns, A. Dias, P. Miller, T.M. Ward, S. Dean, J. Clarke, A. Campion-Flora, D.N. Rodrigues, J.S. Reis-Filho, J.M. Rae, D. Thomas, D. Berry, D. El-Ashry, M.E. Lippman, Infiltrating S100A8+ myeloid cells promote metastatic spread of human breast cancer and predict poor clinical outcome, Breast Cancer Res. Treat. 148 (1) (2014) 41–59, https://doi.org/10.1007/s10549-014-3122-4.
[12] S. Hiratsuka, S. Ishibashi, T. Tomita, A. Watanabe, S. Akashi-Takamura, M. Murakami, K. Kijima, K. Miyake, H. Aburatani, Y. Maru, Primary tumours modulate innate immune signalling to create pre-metastatic vascular hyperpermeability foci, Nat. Commun. 4 (2013) 1853, https://doi.org/10.1038/ncomms2856.
[13] B. Chen, A.L. Miller, M. Rebelatto, Y. Brewah, D.C. Rowe, L. Clarke, M. Czapiga, K. Rosenthal, T. Imamichi, Y. Chen, C.S. Chang, P.S. Chowdhury, B. Naiman,

Y. Wang, D. Yang, A.A. Humbles, R. Herbst, G.P. Sims, S100A9 induced inflammatory responses are mediated by distinct damage associated molecular patterns (DAMP) receptors in vitro and in vivo, PLoS One 10 (2) (2015) e0115828, , https://doi.org/10.1371/journal.pone.0115828.

[14] Y. Fu, Z. Xin, B. Liu, J. Wang, J. Wang, X. Zhang, Y. Wang, F. Li, Platycodin D inhibits inflammatory response in LPS-stimulated primary rat microglia cells through activating LXRalpha-ABCA1 signaling pathway, Front. Immunol. 8 (2017) 1929, https://doi.org/10.3389/fimmu.2017.01929.

[15] Y. Qu, L. Zhou, C. Wang, Effects of platycodin D on IL-1beta-induced inflammatory response in human osteoarthritis chondrocytes, Int. Immunopharmacol. 40 (2016) 474–479, https://doi.org/10.1016/j.intimp.2016.09.025.

[16] B. Wang, Y. Gao, G. Zheng, X. Ren, B. Sun, K. Zhu, H. Luo, Z. Wang, M. Xu, Platycodin D inhibits interleukin-13-induced the expression of inflammatory cytokines and mucus in nasal epithelial cells, Biomed. Pharmacother. 84 (2016) 1108–1112, https://doi.org/10.1016/j.biopha.2016.10.052.

[17] T. Li, X. Chen, X. Chen, D.L. Ma, C.H. Leung, J.J. Lu, Platycodin D potentiates proliferation inhibition and apoptosis induction upon AKT inhibition via feedback blockade in non-small cell lung cancer cells, Sci. Rep. 6 (2016) 37997, https://doi.org/10.1038/srep37997.

[18] H. Imamura, S. Takao, T. Aikou, A modified invasion-3-(4,5-dimethylthiazole-2-yl)-2,5-diphenyltetrazolium bromide assay for quantitating tumor cell invasion, Cancer Res. 54 (13) (1994) 3620–3624.

[19] M. Pruenster, A.R. Kurz, K.J. Chung, X. Cao-Ehlker, S. Bieber, C.F. Nussbaum, S. Bierschenk, T.K. Eggersmann, I. Rohwedder, K. Heinig, R. Immler, M. Moser, U. Koedel, S. Gran, R.P. McEver, D. Vestweber, A. Verschoor, T. Leanderson, T. Chavakis, J. Roth, T. Vogl, M. Sperandio, Extracellular MRP8/14 is a regulator of beta2 integrin-dependent neutrophil slow rolling and adhesion, Nat. Commun. 6 (2015) 6915, https://doi.org/10.1038/ncomms7915.

[20] X. Tan, X. Zheng, Z. Huang, J. Lin, C. Xie, Y. Lin, Involvement of S100A8/A9-TLR4-NLRP3 inflammasome pathway in contrast-induced acute kidney injury, Cell. Physiol. Biochem. 43 (1) (2017) 209–222, https://doi.org/10.1159/000480340.

[21] Y. Liu, Y. Gu, Y. Han, Q. Zhang, Z. Jiang, X. Zhang, B. Huang, X. Xu, J. Zheng, X. Cao, Tumor exosomal RNAs promote lung pre-metastatic niche formation by activating alveolar epithelial TLR3 to recruit neutrophils, Cancer Cell 30 (2) (2016) 243–256, https://doi.org/10.1016/j.ccell.2016.06.021.

[22] T. Tomita, Y. Sakurai, S. Ishibashi, Y. Maru, Imbalance of Clara cell-mediated homeostatic inflammation is involved in lung metastasis, Oncogene 30 (31) (2011) 3429–3439, https://doi.org/10.1038/onc.2011.53.

[23] K. Narumi, R. Miyakawa, R. Ueda, H. Hashimoto, Y. Yamamoto, T. Yoshida, K. Aoki, Proinflammatory proteins S100A8/S100A9 activate NK cells via interaction with RAGE, J. Immunol. 194 (11) (2015) 5539–5548, https://doi.org/10.4049/jimmunol.1402301.

[24] Y. Wang, Z. Zhang, L. Zhang, X. Li, R. Lu, P. Xu, X. Zhang, M. Dai, X. Dai, J. Qu, F. Lu, Z. Chi, S100A8 promotes migration and infiltration of inflammatory cells in acute anterior uveitis, Sci. Rep. 6 (2016) 36140, https://doi.org/10.1038/srep36140.

[25] C.H. Kwon, H.J. Moon, H.J. Park, J.H. Choi, D.Y. Park, S100A8 and S100A9 promotes invasion and migration through p38 mitogen-activated protein kinase-dependent NF-kappaB activation in gastric cancer cells, Mol. Cell 35 (3) (2013) 226–234, https://doi.org/10.1007/s10059-013-2269-x.

[26] Y. Carmi, S. Dotan, P. Rider, I. Kaplanov, M.R. White, R. Baron, S. Abutbul, M. Huszar, C.A. Dinarello, R.N. Apte, E. Voronov, The role of IL-1beta in the early tumor cell-induced angiogenic response, J. Immunol. 190 (7) (2013) 3500–3509, https://doi.org/10.4049/jimmunol.1202769.

[27] K.O. Osuala, M. Sameni, S. Shah, N. Aggarwal, M.L. Simonait, O.E. Franco, Y. Hong, S.W. Hayward, F. Behbod, R.R. Mattingly, B.F. Sloane, Il-6 signaling between ductal carcinoma in situ cells and carcinoma-associated fibroblasts mediates tumor cell growth and migration, BMC Cancer 15 (2015) 584, https://doi.org/10.1186/s12885-015-1576-3.

[28] A. Maolake, K. Izumi, A. Natsagdorj, H. Iwamoto, S. Kadomoto, T. Makino, R. Naito, K. Shigehara, Y. Kadono, K. Hiratsuka, G. Wufuer, K.L. Nastiuk, A. Mizokami, Tumor necrosis factor-alpha induces prostate cancer cell migration in lymphatic metastasis through CCR7 upregulation, Cancer Sci. 109 (5) (2018) 1524–1531, https://doi.org/10.1111/cas.13586.

[29] J. Chun, Y.S. Kim, Platycodin D inhibits migration, invasion, and growth of MDA-MB-231 human breast cancer cells via suppression of EGFR-mediated Akt and MAPK pathways, Chem. Biol. Interact. 205 (3) (2013) 212–221, https://doi.org/10.1016/j.cbi.2013.07.002.